

# TISE: A Toolbox for Text-to-Image Synthesis Evaluation

Tan M. Dinh

Rang Nguyen

Binh-Son Hua

VinAI Research, Vietnam

## Abstract

In this paper, we conduct a study on state-of-the-art methods for single- and multi-object text-to-image synthesis and propose a common framework for evaluating these methods. We first identify several common issues in the current evaluation of text-to-image models, which are: (i) a commonly used metric for image quality assessment, e.g., Inception Score (IS), is often either miscalibrated for the single-object case or misused for the multi-object case; (ii) the overfitting phenomenon appears in the existing R-precision (RP) and SOA metrics, which are used to assess text relevance and object accuracy aspects, respectively; (iii) many vital factors in the evaluation of the multi-object case are primarily dismissed, e.g., object fidelity, positional alignment, counting alignment; (iv) the ranking of the methods based on current metrics is highly inconsistent with real images. Then, to overcome these limitations, we propose a combined set of existing and new metrics to systematically evaluate the methods. For existing metrics, we develop an improved version of IS named IS\* by using temperature scaling to calibrate the confidence of the classifier used by IS; we also propose a solution to mitigate the overfitting issues of RP and SOA. Regarding a set of new metrics compensating for the lacking of vital evaluating factors in the multi-object case, we develop CA for counting alignment, PA for positional alignment, object-centric IS (O-IS), object-centric FID (O-FID) for object fidelity. Our benchmark, therefore, results in a highly consistent ranking among existing methods, being well-aligned to human evaluation. We also create a strong baseline model (AttnGAN++) for the benchmark by a simple modification from the well-known AttnGAN. We will release this toolbox for unified evaluation, so-called TISE, to standardize the evaluation of the text-to-image synthesis models. The project page for TISE can be found [here](#).

## 1. Introduction

The unprecedented growth of deep learning has sparked significant interest in solving the vital vision-language task of text-to-image synthesis in recent years, with potential ap-









Caption	DM-GAN	CPGAN	AttnGAN++	Real Images
Several plates of food include fry dough and salad.				
There are people standing on the sand at the beach.				
<b>Inception Score</b>	32.43	52.90	40.13	37.71
<b>R-Precision</b>	92.23	93.59	96.39	67.35
<b>SOA-C</b>	33.44	77.02	48.33	74.97
<b>SOA-I</b>	48.03	84.55	67.19	80.84

Figure 1. **Evaluating the text-to-image synthesis models is a challenging task.** Many existing metrics are inconsistent especially for the case when an input sentence involves multiple objects. Values in red denote inconsistent evaluations, where the quantitative results are even higher than that of real photos, despite the fact that such generated images are not perceptually real.

plications from computer-aided design, image editing with text-guided to image retrieval. This task is challenging because of the wide semantic gap between two domains and highly many-to-many mapping (e.g., one text caption can correspond to many image counterparts and vice versa). Many aspects of image synthesis, such as image fidelity, object relations, object counting have to be considered for generating complex scenes from a sentence or paragraph.

In the past few years, Generative Adversarial Networks (GANs) [7] had obtained tremendous achievements on image synthesis in many domains (e.g. synthesizing human face images [18, 19], or face editing [45, 46]). GANs also show their potential for generating images conditioned on their text captions. Most of text-to-image synthesis approaches [23, 24, 48, 54, 56, 62] are built upon GAN and jointly consider text and image features for synthesis.

Despite excellent results have been achieved on particular datasets [26, 34, 52], the current evaluation pipeline is not perfect. For single object case, image quality and text-image alignment are primary factors considered in a typical evaluation process. Some commonly evaluation metrics are Inception Score (IS) [44] and the Fréchet Inception Distance

(FID) [11] for image fidelity and R-precision (RP) [54] for text-image alignment, which works well for most single-object cases. However, in complex scenes with multiple objects, adopting these metrics are not enough and causes some inconsistency issues. As can be seen in Figure 1, the ranking of GANs model based on the current metrics is not strongly correlated to their generated image qualities. The numbers reported from several GANs are even better than the one of corresponding real images, while it is clearly seen that the quality of generated images are still far from being real. Additionally, the existing evaluation system lacks the metrics for assessing other aspects like object fidelity, positional alignment, and counting alignment, among others. These aspects are very vital in accessing the performance of text-to-image models in the multi-object case. Furthermore, the lack of a unified toolbox for evaluation has resulted in inconsistent results reported by different research works. These issues are also highlighted in the recent comprehensive survey [6], which raises a demand to devise a unified text-to-image evaluation framework.

In this paper, we develop a systematic method for evaluating text-to-image synthesis approaches to tackle the challenges mentioned above. Our contributions are summarized as follows:

- In terms of enhancing existing metrics, we create an improved version of IS metric, which helps alleviate the low confidence of original IS due to the miscalibrated pre-trained classifier. Furthermore, we also develop the robust versions for two existing metrics (RP and SOA [12]) to mitigate their overfitting issues in the multi-object case.
- Regarding the new metrics for the multi-object case, we develop O-IS and O-FID for object fidelity, PA for positional alignment, and CA for counting alignment.
- Basing on these metrics, we conduct a comprehensive and fair assessment of current state-of-the-art methods for both single- and multi-object text-to-image models.
- Finally, we offer AttnGAN++, a strong baseline that works well for both single- and multi-object scenarios and has competitive performance to current state-of-the-art text-to-image synthesis models.

On top of these contributions, we develop a Python assessment toolbox as well as a set of practical guidelines to advocate fair comparisons and repeatable outcomes in future text-to-image synthesis research.

## 2. Background

**Text-to-Image Synthesis** is a vision-language task substantially benefit from the unprecedented evolutions of generative adversarial neural networks and language models. GAN-INT-CLS [42] is the first conditional GAN [29] designed

for text-to-image generation, but images generated by GAN-INT-CLS only have  $64 \times 64$  resolution. StackGAN and its successor StackGAN++ [57, 58] enhanced the resolution of generated images by using a multi-stage architecture. These works, however, only consider sentence-level features for image synthesis; word-level features are completely dismissed, which causes poor image details. To fix this issue, an attention mechanism can be used to provide word-level features, notably used by AttnGAN [54] and DM-GAN [62], which significantly improves the generated image quality. Beyond modifying the network architecture, improving semantic consistency between image and caption is also an active research topic to gain better image quality. SD-GAN [56] and SE-GAN [48] guarantee text-image consistency by the Siamese mechanism while [36] proposes a text-to-image-to-text framework called MirrorGAN inspired by the cycle consistency. [55, 60] leverage contrastive learning in their text-to-image models. Recently, DALL-E [39] is a large scale text-to-image model with 12 billion parameters synthesizing image from caption autoregressively by using a transformer [51] and VQ-VAE [40] with the support from a strong text-image matching model CLIP [38].

**Evaluation.** The rapid advancement of text-to-image generation necessitates the construction of a reliable and systematic evaluation framework to benchmark models and guide future research. However, assessing the quality of generative modeling tasks has proven difficult in the past. [50]. Because none of the existing measures are perfect, it is usual to report many metrics, each of which assesses a different aspect. The performance assessment is even more challenging in the text-to-image synthesis task due to the multi-modal complexity of text and image, which motivates us to develop a new evaluation toolbox to compare text-to-image approaches fairly and confidently.

## 3. Single-Object Text-to-Image Synthesis

### 3.1. Existing Metrics

Most of existing metrics access the quality of model based on two aspects: image quality and text-image alignment. For assessing the image quality of the model, Inception score (IS) [44] and Fréchet Inception Distance (FID) [11] are two common metrics. These metrics originally come from traditional generative modeling tasks for evaluating quality of single-object image sets. For evaluating text-image alignment, R-precision [54] metric is utilized popularly.

**Inception Score (IS)** [44] is a non-reference metric that leverages a pretrained Inception-v3 network [47] for calculating the Kullback-Leibler divergence (KL-divergence) between class-conditional distribution and class-marginal distribution. The formula of IS is defined below.

$$IS = \exp(\mathbb{E}_x D_{KL}(p(y|x) \parallel p(y))), \quad (1)$$

where  $x$  is the generated image and  $y$  is the class label. The goal of this metric is to determine whether a decent generator can generate samples under two conditions: (i) The object in the image should be *distinct*  $\rightarrow p(y|x)$  must have low entropy; (ii) Generated images should have the *diversity* of object class  $\rightarrow p(y)$  must have high entropy. Combining these two considerations, we expect that the KL-divergence between  $p(y)$  and  $p(y|x)$  should be large. Therefore, higher IS value means better image quality and diversity.

**Fréchet Inception Distance (FID)** [11] is a referenced metric that calculates the Fréchet distance between two sets of images: generated and actual. To calculate FID, features from each set are firstly extracted by a pre-trained Inception-v3 network [47]. Then, these two feature sets are modeled as two *multivariate Gaussian distributions*. Finally, the Fréchet distance is calculated between two distributions.

$$\text{FID} = \|\mu_r - \mu_g\|^2 + \text{trace} \left( \Sigma_r + \Sigma_g - 2(\Sigma_r \Sigma_g)^{\frac{1}{2}} \right), \quad (2)$$

where  $X_r \sim \mathcal{N}(\mu_r, \Sigma_r)$  and  $X_g \sim \mathcal{N}(\mu_g, \Sigma_g)$  are the features of real images and generated images extracted by a pretrained Inception-v3 model. Lower FID value means better image quality and diversity.

**R-precision (RP)** [54] metric is used popularly to evaluate text-image consistency. The idea of RP is to use synthesized image query again the input caption. In particular, given a ground truth text description and 99 mismatching captions sampled randomly, an image is generated from ground truth caption. Then this image is used to query again input description among 100 candidate captions. This retrieval is marked as successful if the matching score of it and ground truth caption is the highest one. The cosine similarity between image encoding vector and caption encoding vector is used as matching score. RP is the ratio of successful retrieval and higher score means better quality.

### 3.2. Benchmark Results

To further study the performance of the metrics, we conduct an assessment to re-evaluate existing works in single-object text-to-image synthesis. For simplicity, CUB dataset [52] is selected for our mini-benchmark and used to generate images with only one object from fine-grained text description. CUB dataset [52] contains 11,788 images from 200 different bird species. We firstly pre-process images from CUB dataset as the same way described in [57] to remove some irrelevance contents with caption such as background and further help model to focus on generate an object in the image. In order to evaluate the generalization capability of methods, all the models are trained with zero-shot setting, particularly, 150 bird classes for training and 50 other bird classes for testing.

Method	IS ( $\uparrow$ )	FID ( $\downarrow$ )	RP ( $\uparrow$ )
GAN-INT-CLS [42]	2.73	194.41	3.83
StackGAN++ [58]	4.10	27.40	13.57
AttnGAN [54]	4.32	24.27	65.30
AttnGAN + CL [55]	4.45	17.96	60.82
DM-GAN [62]	4.68	15.52	<u>76.25</u>
DF-GAN [49]	4.75	21.31	39.03
DM-GAN + CL [55]	<u>4.77</u>	<b>14.57</b>	69.80
AttnGAN++ (ours)	<b>4.78</b>	<u>15.01</u>	<b>77.32</b>

Table 1. **Benchmark results for the single-object text-to-image synthesis models on the CUB dataset.** In this benchmark, we only consider the methods, which have been released with officially source code and pre-trained weights by their authors. **Best** and runner-up values are marked in bold and underline.

We suggest a new baseline approach for this benchmark based on recent breakthroughs in deep learning techniques, in addition to previous efforts. Particularly, we revise the architecture of AttnGAN [54] by adding the spectral normalization layers to the discriminator that helps stabilize the training process. We also hand-tune the hyperparameters of our baseline network, which we denote as AttnGAN++. The detail architecture and network setting of AttnGAN++ are shown in supplementary material. The quantitative results of our benchmark is reported in Table 1, which brings the following insights.

**Insight 1: AttnGAN++ is a strong baseline.** As can be seen in Table 1, our AttnGAN++ outperforms the original version (AttnGAN) with a large gap on all metrics for CUB dataset and has the comparable results with existing state-of-the-art works. It is worth noting that most of current state-of-the-art works [22, 24, 55, 62] are built on AttnGAN. Therefore, this empirical finding would help create a very strong baseline for further improving the successor works. The qualitative results can be found in the supplementary.

**Insight 2: IS scores are inconsistent.** During the development of AttnGAN++, we discovered that it is feasible to design a generator that produces unrealistic images while yet having a high IS score, which we refer to as the *counter model*. Generated images from this counter model is shown in Figure 2(a). Note that the images from the counter model are randomly sampled and not curated. We describe the architecture of this counter model as well as how to reproduce these results in the supplementary.

Motivated by Insight 2, we revisited the definition of IS metric, and discovered that the inconsistency is due to a pitfall when the IS score is computed in the text-to-image synthesis task. From this observation, we proposed an im-

proved version of IS that address such limitation, as follows.

### 3.3. Improved Inception score (IS\*): Calibrating Image Classifiers

We found that the pretrained classifier based on the Inception network (used to calculate IS) is uncalibrated or mis-calibrated. As a result, the classifier tends to be either over-confident or under-confident. This is verified by using expected calibration error (ECE) [32] and reliability diagram [5, 33]. ECE is the popular metric used to evaluate calibration whereas reliability diagram is a tool to visualize calibration quality. A classifier is well calibrated if they have a small ECE value and reliability diagram is close to identity. As can be seen in Figure 3(a), the Inception network, pretrained by StackGAN [57] for evaluating recent text-to-image models on CUB, is under-confident. When computing the IS, this leads to inconsistency due to erroneous distance between conditional and marginal probability distributions.

To tackle this issue, we propose to calibrate the confidence score of the classifier, which we opt to apply the popular network calibration method of temperature scaling [9]. Particularly, the classifier receives an input image  $x$  and output a logit vector  $z$ . Before this logit vector  $z$  is passed to a softmax layer to obtain probability values, we calibrate  $z$  by scaling it with a positive scalar value  $T$  for all classes. The conditional probability  $p(y = k | x)^*$  with class label  $k \in \{1..K\}$  after calibration is:

$$p(y = k | x)^* = \sigma(z/T)_k, \quad (3)$$

where  $K$  is the number of classes,  $T$  is the temperature, and  $\sigma$  represents the softmax function. We use the  $p(y | x)^*$  vector for computing the divergence in IS\*. The calibrated confidence score is  $\max_k p(y = k | x)^*$ .

The value of  $T$  is obtained by optimizing the negative log-likelihood loss on the validation set used to train the classifier. After calibration on CUB, we get  $T = 0.598$ . Figure 3(b) showed that after calibration, the under-confident issue is greatly mitigated illustrated by a significant drop in ECE error and a nearly diagonal shape of the plot. The IS\* score shown in Table 2 demonstrated that the inconsistent score causing by the countermodel is also addressed by using IS\* instead of IS.

Furthermore, we also conduct another experiment to verify the impact of the calibration step causing on computing IS\*. In detail, this experiment is performed on the vanilla GAN task, which is the Tiny ImageNet [21] image generation. The classifier used to measure IS in these works is the Inception-v3 network pre-trained on ImageNet [43]. It is worth noting that this classifier is used popularly for measuring IS in the traditional GAN image generation task. The IS and IS\* results are shown in Table 3. We also plot the reliability diagrams and ECE errors of this classifier before and after calibration in Figure 4. Even before calibration,



(a) IS = 5.12; IS\* = 13.05 (b) IS = 4.78; IS\* = 15.13

Figure 2. **Evaluating the single-object text-to-image synthesis models can be inconsistent with the IS score.** (a) Generated images from the counter model are unrealistic but the IS score of this model is high; (b) Generated images of our AttnGAN++. As can be seen, our IS\* fixes well this inconsistency issue.

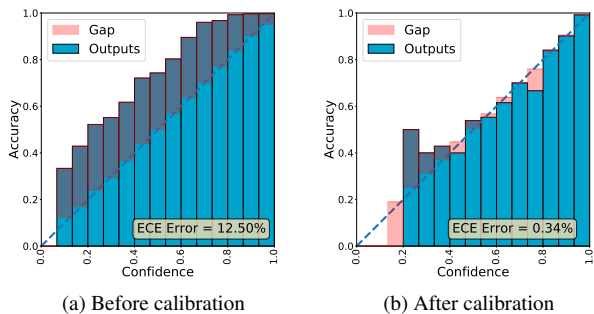


Figure 3. Reliability diagrams of the fine-tuned Inception-v3 network on the CUB dataset before and after calibration.

this classifier is noticeably well calibrated. Hence, the effect of the calibration process on this classifier is negligible in comparison with the significant effect they cause in the CUB dataset mentioned above since the temperature  $T$  after calibration is 0.909 ( $T = 1$  means calibration does not have any effects on classifier). Therefore, we would only see the local ranking differs in IS and IS\*.

**Summary.** Single-object text-to-image synthesis on image datasets such as CUB dataset can be solved effectively using existing method. FID, RP and our IS\* are good metrics for evaluating the quality of generated images. So far, the problem is limited on datasets of a single object type, e.g., bird in CUB [52] or flower in Oxford [34]. Developing new models for generating single objects but with multiple categories would be an interest future work.

## 4. Multiple-Object Text-to-Image Synthesis

Notwithstanding the success of single-object text-to-image synthesis, generating complex images with many ob-

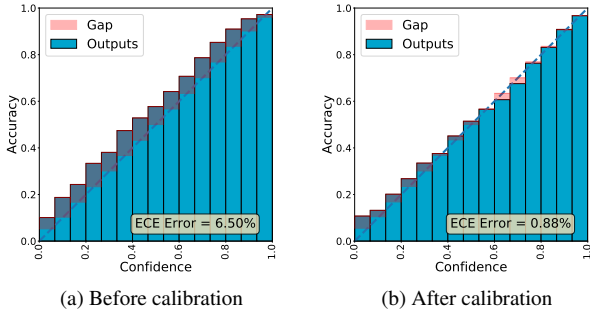


Figure 4. Reliability diagrams of the Inception-v3 network pre-trained on the ImageNet dataset before and after calibration.

Method	IS ( $\uparrow$ )	IS* ( $\uparrow$ )
GAN-INT-CLS [42]	2.73	7.51
StackGAN++ [58]	4.10	12.69
HDGAN [61]	4.17	13.12
AttnGAN [54]	4.32	13.63
AttnGAN + CL [55]	4.45	14.42
DM-GAN [62]	4.68	15.00
DF-GAN [49]	4.75	14.79
DM-GAN + CL [55]	4.77	<u>15.08</u>
Counter Model	<b>5.12</b>	13.05
AttnGAN++ (ours)	<u>4.78</u>	<b>15.13</b>
<i>Real Images</i>	<i>24.16</i>	<i>46.27</i>

Table 2. A comparison between the IS and IS\* scores on the CUB dataset. Thanks to the calibration of the image classifier, our IS\* no longer suffers the problem of counter models being ranked high despite producing bad results.

Method	IS ( $\uparrow$ )	IS* ( $\uparrow$ )
WGAN-GP [8]	1.64	1.79
GGAN [25]	5.22	7.00
LSGAN [28]	5.39	7.36
DCGAN [37]	5.70	7.79
ProjGAN [30]	6.19	8.64
ACGAN [35]	6.51	9.30
BigGAN-LO [53]	7.83	11.29
SNGAN [31]	<b>8.38</b>	<b>12.36</b>
SAGAN [59]	<b>8.48</b>	<b>12.34</b>
WGAN-DRA [20]	9.35	14.00
BigGAN [1]	12.43	18.80
ContraGAN [15]	13.76	21.64

Table 3. Comparing the ranking of IS and IS\* on Tiny ImageNet dataset with various GAN models. The cases, which are ranked inconsistently between IS and IS\*, are marked in **bold**. As we expect, only local ranking differs between IS and IS\* appear due to the well-calibrated of the classifier even before calibration.

Metric	Image Realism	Object Fidelity	Text Relevance	Object Accuracy	Positional Alignment	Counting Alignment	Paraphrase Robustness	Explainable	Automatic
IS [44]	✓								✓
FID [11]	✓								✓
RP [54]			✓						✓
SOA [12]			✓	✓					✓
O-IS (Ours)		✓							✓
O-FID (Ours)		✓							✓
PA (Ours)					✓				✓
CA (Ours)						✓			✓
Human	✓	✓	✓	✓	✓	✓	✓	✓	✓

Table 4. Demanding aspects for the evaluation of multi-object text-to-image synthesis models presented by [6] and our proposed metrics to assess the lacking criteria.

jects from a single sentence is a great challenge and unsolved problem. InferGAN [13] and Obj-GAN [23] handle this by introducing a two-step generation process including layout generation and image generation. Recently, CPGAN [24] leverages the object memory features helping for boosting the performance of the multi-object text-to-image synthesis models significantly.

Regarding the evaluation, simply using existing metrics as in single-object text-to-image synthesis does not perform well since the generated images contain multiple objects, e.g., a couple of men riding horses on top of a green field. Several crucial aspects have been implied or ignored in the current evaluation metrics such as object count, relative position among objects, etc. In this section, we will describe a systematic approach for evaluating the quality of the generated images contain multiple objects more accurately.

The comprehensive survey in the concurrent work by [6], which suggested many aspects for evaluating a method for multiple-object text-to-image synthesis. We summarize these aspects in Table 4. According to their work, positional alignment measures the relative position among the objects in the image, e.g., when there is a man and a tree in an image, whether ‘a man stands in front of a tree’ and ‘a man stands behind a tree’ affects the positional alignment. Counting alignment measures the compatibility on the number of objects illustrated by the input sentence and the generated image. Unfortunately, [6] simply offers a discussion of such issues without proposing any concrete metrics for an actual assessment. In contrast, we propose in this paper two new metrics namely PA for positional alignment and CT for counting alignment to evaluate these aspects.

Let us now detail all metrics in our toolbox for evaluating multiple-object text-to-image synthesis, below. Our benchmark is conducted on the MS-COCO dataset [26], which contains photos with many objects and complex backgrounds. The setup for preparing training and validation set in our experiments are same with [42]. We specifically use MS-COCO version 2014, the training set of text-to-image models is the official training set of MS-COCO (approximately 80K images), and we test models on the MS-COCO validation set (approximately 40K images).

#### 4.1. Existing Metrics

**Image Realism.** FID and our IS\* can be used to analyze the photorealism of multi-object synthetic images in the same way they have been used for single object images.

**Text Relevance.** Current studies use RP to assess the alignment between text and the generated image. However, this metric is shown to overfit in multiple-object synthesis, having inconsistent ranking with real images, which can be seen in Figure 1. One reason for this is that previous works have used the same image and text encoders for training and computing RP. To alleviate overfitting issue, we use an independent text encoder and image encoder for RP. We selected CLIP [38], a powerful text and image encoders trained on a very large-scale dataset with 400 million text-image pairs. In our experiment, the overfitting problem of RP is mitigated using two new encoders, as demonstrated by the value of RP in real images have a large gap with the previous methods. A comparison between the traditional and our modified RP results can be found in supplementary material.

**Object Accuracy.** Semantic Object Accuracy (SOA) [12] is proposed to measure whether generate images having the objects mentioned in the caption. Specifically, the authors proposed two sub-metrics including SOA-I (average recall between images) and SOA-C (average recall between classes), which are formulated as:

$$\text{SOA-C} = \frac{1}{|C|} \sum_{c \in C} \frac{1}{|I_c|} \sum_{i_c \in I_c} \text{Obj-Det}(i_c), \quad (4)$$

$$\text{SOA-I} = \frac{1}{\sum_{c \in C} |I_c|} \sum_{c \in C} \sum_{i_c \in I_c} \text{Obj-Det}(i_c), \quad (5)$$

where  $C$  is the object category set;  $I_c$  is a set of images belonging to category  $c$ ;  $\text{Obj-Det}(i_c) \in \{0, 1\}$  is a pretrained object detector returning 1 if the detector detect successfully an object belong to class  $c$  in  $i_c$ .

As can be seen, SOA is a plausible metric to evaluate the object accuracy factor in the text-to-image model. However, we found that both CPGAN [24] and SOA used the same pre-trained YOLO-v3 [41] in their implementation, which can potentially lead to overfitting. Empirically, the values of SOA-I and SOA-C of CPGAN are better than those

for real images despite images from CPGAN are still non-realistic (Figure 1). To lessen the chance of overfitting, we choose Mask-RCNN [10] instead of YOLO-v3 to compute SOA. The empirical result in our experiment shows that this selection helps mitigate the inconsistency problem. A comparison between the SOA results when using YOLO-v3 and Mask-RCNN can be found in the supplementary material. In this paper, we solely report SOA values computed by Mask-RCNN.

As discussed in Table 4 and inspired by [6], several aspects in evaluating multiple-object text-image synthesis are not well studied. In the following sections, let us devise additional metrics to handle the current image-based unsolved aspects including *Object Fidelity*, *Positional Alignment* and *Counting Alignment*.

#### 4.2. Object Fidelity

Object-centric IS (O-IS) and Object-centric FID (O-FID) are our straightforward extensions of IS and FID with the aim to measure object fidelity in a generated image. Specifically, we first use an object detector to localize and crop all object regions in each image in the generated image set. By treating all image regions as independently generated, we evaluate the fidelity by IS\* and FID on the image regions, respectively. In our experiments, we used Mask-RCNN [10] pre-trained on MS-COCO as the object detector. We also fine-tune Inception-v3 classifier on the object dataset cropped from the images in MS-COCO dataset based on ground truth bounding boxes to obtain a classifier having 80 classes, equaling the number of classes in MS-COCO. The Inception-v3 network after fine-tuning is used for both computing O-IS and O-FID.

#### 4.3. Positional Alignment

Text descriptions are used to describe an image and typically include phrases that convey the positioning information between objects, such as *behind*, *on top of*, *etc* (Figure 5). However, existing object-aware metrics like SOA do not penalize such incorrect relative object locations (e.g. generated images with inaccurate positional alignment still has high SOA scores). To tackle this issue, we propose a new metric to evaluate positional alignment, denoted by PA. First, we define the set of positional words as  $W = \{\textit{above}, \textit{right}, \textit{far}, \textit{outside}, \textit{between}, \textit{below}, \textit{on top of}, \textit{bottom}, \textit{left}, \textit{inside}, \textit{in front of}, \textit{behind}, \textit{on}, \textit{near}, \textit{under}\}$ . For each word  $w$  in  $W$ , we filter the captions having word  $w$  in the evaluation set of the COCO dataset, and obtain the caption set  $P_w$  for each word  $w$ . Each caption in  $P_w$  is a matched caption, which means the image clearly explains the text. Given  $P_w$ , we build a mismatched caption by replacing  $w$  in the matched caption by its antonym and keeping other words. For example, the mismatched caption of "A man is *in front of* the blue car" is "A man is *behind* the blue car". Our evaluation



Figure 5. **Assessing positional alignment of the objects in the multi-object image is critical, yet it is still mostly ignored.** This example shows a flaw in the existing metrics, such as SOA, which completely ignored the evaluation of positional alignment while maintaining good object accuracy. As can be seen, the SOA values for the image with the *true* caption and with the *false* caption are the same, which demonstrates that the SOA metric skips positional alignment criteria. This weakness leads to the appearance of our Positional Alignment (PA) metric.

begins by generating images from the matched captions in the test dataset. For each word  $w$  in  $W$ , we now have a set  $D_w = \{(R_{wi}, P_{wi}, Q_{wi})\}_{i=1}^{N_w}$  where  $R_{wi}$  is a generated image from  $P_{wi}$ ;  $P_{wi}$  is matched caption;  $Q_{wi}$  is mismatched caption of  $P_{wi}$ ;  $N_w$  is the number of captions having word  $w$ . For each triplet in  $D_w$ , we use the image  $R_{wi}$  to query the input caption from the binary query set including matched caption  $P_{wi}$  and mismatched caption  $Q_{wi}$ . We mark a query as successful if the matched caption is successfully queried. The query success rate measures the positional alignment quality over all words:

$$PA = \frac{1}{|W|} \sum_{w \in W} \frac{k_w}{N_w}, \quad (6)$$

where  $k_w$  is the number of success cases, and  $|W|$  is the total number of words. For image-to-text query, we use CLIP [38] as our text-image matching model.

#### 4.4. Counting Alignment

In the multi-object case, counting alignment is an vital factor but so far disregarded in current text-to-image synthesis evaluation. Therefore, we propose a metric for counting alignment (CA metric) that measures how closely the number of objects in a generated image matches the text description.

To evaluate with CA, we first need to construct the test data by filtering from captions in MS-COCO validation set the captions mentioned counting aspect such as *a*, *one*, *two*, *three*, *four*. From these selected captions, we annotate the ground truth counting information for each one. It is worth noting that we only annotate the object types which can be counted by an object counter to avoid this metric to penalizing those object categories, which cannot be counted. For example, with a caption "A group of seven people having a

*light meal and discussion at a single large table*", the ground truth counting is  $\{ "person": 7.0, "dining table": 1.0 \}$ . Finally, we created a counting test set  $D$  with 1000 records. Each record has a form of  $(t, c)$ , in which  $t$  is an input text description, and  $c$  is the ground truth counting information.

We use a text-to-image model to generate images from each caption and use an off-the-shelf object counting model [3] to count the number of objects for each object class from generated images. To get CA value, we compare the object count to the ground truth and measure the counting error using root mean squared error averaged over the test images:

$$CA = \frac{1}{|D|} \sum_{i=1}^{|D|} \sqrt{\frac{1}{N_{ic}} \sum_{j=1}^{N_{ic}} (\hat{c}_{ij} - c_{ij})^2}, \quad (7)$$

where  $c_{ij}$  and  $\hat{c}_{ij}$  is the ground truth and predicted object count in the image  $i$  for object class  $j$ ;  $N_{ic}$  is the number of ground truth object types in image  $i$ ,  $|D|$  is the number of test samples.

#### 4.5. Ranking Score

To facilitate the benchmark, we propose a simple formula to compute an average score for ranking purpose. The ranking score is calculated by summing all rankings of the considered metrics. To the best of our knowledge, a similar approach is used in the nuScenes challenge for autonomous driving [2] that ranks object detection methods by combining metrics for different bounding box properties such as center, orientation, and dimensions. In our case, since some evaluation aspects could have more than one metric variant, the score for each aspect is the average of scores from the variants. We use  $\frac{1}{2}$  weight for IS and FID in image realism, O-IS and O-FID in object fidelity, SOA-I and SOA-C in object accuracy; other metrics have a unit weight. Our ranking score (RS) is computed as

$$RS = \frac{1}{2}(\#IS^* + \#FID) + \frac{1}{2}(\#O-IS + \#O-FID) \quad (8)$$

$$+ \frac{1}{2}(\#SOA-I + \#SOA-C) + \#PA + \#CA + \#RP,$$

where  $\#(\text{metric}) \in \{1..N\}$  denotes the ranking by a particular metric with  $N$  is the number of considered methods.

#### 4.6. Benchmark Results

We show results of our benchmark in Table 5, from which we draw some following insights. Firstly, our proposed metrics (O-IS, O-FID, CA, PA) and two improved version of existing metrics (RP, SOA), properly rank real images as the best. An exception is IS\* which ranks AttnGAN++ and CPGAN better than real images. However we opt to retain this metric due to its excellent properties on the single-object case, and the ranking score is consistent to human

Method	IS* (↑)	FID (↓)	RP(↑)	SOA-C(↑)	SOA-I (↑)	O-IS (↑)	O-FID (↓)	CA (↓)	PA (↑)	RS (↑)
GAN-CLS [42]	8.10	192.09	10.00	5.31	5.71	2.46	51.13	2.51	32.79	7.0
StackGAN [57]	15.50	53.44	9.10	9.24	9.90	3.36	29.09	2.41	34.33	11.5
AttnGAN [54]	33.79	36.90	50.56	47.13	49.78	5.04	20.92	1.82	40.08	29.5
DM-GAN [62]	45.63	28.96	66.98	55.77	58.11	5.22	17.48	1.71	42.83	41.0
CPGAN [24]	<b>59.64</b>	50.68	69.08	<b>81.86</b>	<b>83.83</b>	<b>6.38</b>	20.07	2.07	43.28	43.0
DF-GAN [49]	27.59	28.73	37.26	33.54	36.00	4.80	17.42	1.92	40.91	27.5
AttnGAN + CL [55]	36.85	26.93	57.52	47.45	49.33	4.92	19.92	1.72	43.92	38.0
DM-GAN + CL [55]	46.61	<b>22.60</b>	<u>70.36</u>	58.68	61.05	5.09	<u>15.50</u>	<u>1.66</u>	<b>49.06</b>	<u>53.0</u>
DALLE-mini (zero-shot) [4]	19.82	62.90	48.72	26.64	27.90	4.10	23.83	2.31	47.39	23.5
AttnGAN++ (Ours)	<u>54.63</u>	<u>26.58</u>	<b>72.50</b>	<u>67.77</u>	<u>69.97</u>	<u>6.02</u>	<b>15.43</b>	<b>1.57</b>	<u>47.75</u>	<b>57.0</b>
<i>Real Images</i>	<i>51.25</i>	<i>2.62</i>	<i>83.54</i>	<i>90.02</i>	<i>91.19</i>	<i>8.63</i>	<i>0.00</i>	<i>1.05</i>	<i>100.0</i>	<i>65.0</i>

Table 5. **Benchmark performances of the multi-object text-to-image synthesis models on the MS-COCO dataset.** The best and runner-up values are marked in bold and underline, respectively. As can be seen, our AttnGAN++ gains the competitive results compared to the current state-of-the-art text-to-image synthesis methods.

when including IS\*. Second, our AttnGAN++ is ranked top for multi-object text-to-image synthesis in terms of overall performance, demonstrating that it is a substantial strong baseline for both single-object and multiple-object instances. Third, breaking down each part of our evaluation pipeline allows us to more clearly analyze each model’s flaws and strengths than earlier evaluations. For examples, CPGAN outperforms other techniques on SOA-I and SOA-C since it explicitly considers object-level information in the training phase. DM-GAN + CL is the most effective method for positional alignment. While our AttnGAN++ performs better in the remaining aspects. The details of aspect’s scores for each method are included in the supplementary material. Finally, it is worth noting that one of the drawbacks of the existing evaluation pipeline is the lack of a unified evaluation tool to calculate the metrics fairly and consistently, and it currently would be solved by our TISE toolbox. TISE implements all above metrics in a unified way, and helps mitigate the weakness of the existing evaluation pipeline.

Method	Ranking Score (↑)	Human Score (↑)
StackGAN [57]	6.00	28.45
AttnGAN [54]	13.5	37.40
DM-GAN [62]	20.0	41.47
CPGAN [24]	23.0	43.73
AttnGAN++ (ours)	<b>28.5</b>	<b>45.01</b>
<i>Real Images</i>	<i>35.0</i>	<i>99.82</i>

Table 6. **Human evaluation results on the MS-COCO dataset.** In this table, ranking scores (RS) are recalculated using just 5 considered techniques and real photos. As can be observed, RS is well-aligned with human decisions.

## 4.7. Human Evaluation

To ensure that our evaluations are reliable, we conducted a user analysis to test the metrics against assessments done by humans. We opt for 5 methods including StackGAN, AttnGAN, DM-GAN, CPGAN, AttnGAN++ (ours), and real images to conduct our user survey. We sample 50 test captions from MS-COCO and use the above methods to generate an image for each caption. The IDs for these captions will be released for reproducibility. We ask each human subject (40 participants in total) to score each method from 1 (worst) to 5 (best) based on two criteria: *plausibility* – whether the image is plausible based on the content of the caption (object accuracy, counting, and positional alignment, text relevance), and *naturalness* – whether the image looks natural. The score of each human subject for each method is the sum of score of 50 images and divide by 250 for normalization. The final score of each method is an average of the scores of each participant. Our evaluation result in Table 6 shows that our final ranking is well-aligned with human evaluation.

## 5. Conclusion

In this paper, we performed an empirical study and benchmarked the text-to-image synthesis methods for both single-object and multiple-object cases. The benchmark results reveal the inconsistency issues in the existing metrics, prompting us to propose the improved version of existing metrics (i.e., IS to IS\*) as well as new metrics to evaluate many vital aspects in the multi-object case, which has been overlooked by previous works (i.e., positional alignment, counting alignment, and object fidelity). Our extensive experiments show that our evaluation toolkit provides a better and more consistent ranking with human evaluation. We would release our TISE toolbox for the community to keep track of the benchmark with future works.



## References

- [1] Andrew Brock, Jeff Donahue, and Karen Simonyan. Large scale gan training for high fidelity natural image synthesis. *arXiv preprint arXiv:1809.11096*, 2018. **5**
- [2] Holger Caesar, Varun Bankiti, Alex H Lang, Sourabh Vora, Venice Erin Liong, Qiang Xu, Anush Krishnan, Yu Pan, Giancarlo Baldan, and Oscar Beijbom. nuscenes: A multimodal dataset for autonomous driving. In *CVPR*, 2020. **7**
- [3] Hisham Cholakkal, Guolei Sun, Fahad Shahbaz Khan, and Ling Shao. Object counting and instance segmentation with image-level supervision. In *CVPR*, 2019. **7**
- [4] Boris Dayma, Suraj Patil, Pedro Cuenca, Khalid Saifullah, Tanishq Abraham, Phuc Le Khac, Luke Melas, and Ritobrata Ghosh. Dall-e mini, 7 2021. URL <https://github.com/borisdayma/dalle-mini>. **8, 13**
- [5] Morris H DeGroot and Stephen E Fienberg. The comparison and evaluation of forecasters. *Journal of the Royal Statistical Society: Series D (The Statistician)*, 32(1-2), 1983. **4**
- [6] Stanislav Frolov, Tobias Hinz, Federico Raue, Jörn Hees, and Andreas Dengel. Adversarial text-to-image synthesis: A review. *arXiv preprint arXiv:2101.09983*, 2021. **2, 5, 6, 11**
- [7] Ian Goodfellow, Jean Pouget-Abadie, Mehdi Mirza, Bing Xu, David Warde-Farley, Sherjil Ozair, Aaron Courville, and Yoshua Bengio. Generative adversarial nets. In *NeurIPS*, 2014. **1**
- [8] Ishaan Gulrajani, Faruk Ahmed, Martin Arjovsky, Vincent Dumoulin, and Aaron Courville. Improved training of wasserstein gans. *arXiv preprint arXiv:1704.00028*, 2017. **5**
- [9] Chuan Guo, Geoff Pleiss, Yu Sun, and Kilian Q Weinberger. On calibration of modern neural networks. *arXiv preprint arXiv:1706.04599*, 2017. **4**
- [10] Kaiming He, Georgia Gkioxari, Piotr Dollár, and Ross Girshick. Mask r-cnn. In *ICCV*, 2017. **6**
- [11] Martin Heusel, Hubert Ramsauer, Thomas Unterthiner, Bernhard Nessler, and Sepp Hochreiter. Gans trained by a two time-scale update rule converge to a local nash equilibrium. In *NeurIPS*, 2017. **2, 3, 5**
- [12] Tobias Hinz, Stefan Heinrich, and Stefan Wermter. Semantic object accuracy for generative text-to-image synthesis. *arXiv preprint arXiv:1910.13321*, 2019. **2, 5, 6**
- [13] Seunghoon Hong, Dingdong Yang, Jongwook Choi, and Honglak Lee. Inferring semantic layout for hierarchical text-to-image synthesis. In *CVPR*, 2018. **5**
- [14] Sergey Ioffe and Christian Szegedy. Batch normalization: Accelerating deep network training by reducing internal covariate shift. *arXiv preprint arXiv:1502.03167*, 2015. **13**
- [15] Minguk Kang and Jaesik Park. Contragan: Contrastive learning for conditional image generation. 2020. **5**
- [16] Animesh Karnewar and Oliver Wang. Msg-gan: Multi-scale gradients for generative adversarial networks. In *CVPR*, 2020. **11**
- [17] Tero Karras, Timo Aila, Samuli Laine, and Jaakko Lehtinen. Progressive growing of gans for improved quality, stability, and variation. *arXiv preprint arXiv:1710.10196*, 2017. **18**
- [18] Tero Karras, Samuli Laine, and Timo Aila. A style-based generator architecture for generative adversarial networks. In *CVPR*, 2019. **1, 18**
- [19] Tero Karras, Samuli Laine, Miika Aittala, Janne Hellsten, Jaakko Lehtinen, and Timo Aila. Analyzing and improving the image quality of stylegan. In *CVPR*, 2020. **1**
- [20] Naveen Kodali, Jacob Abernethy, James Hays, and Zsolt Kira. On convergence and stability of gans. *arXiv preprint arXiv:1705.07215*, 2017. **5**
- [21] Ya Le and Xuan Yang. Tiny imagenet visual recognition challenge. *CS 231N*, 2015. **4**
- [22] Bowen Li, Xiaojuan Qi, Thomas Lukasiewicz, and Philip H. S. Torr. Controllable text-to-image generation. *arXiv preprint arXiv:1909.07083*, 2019. **3**
- [23] Wenbo Li, Pengchuan Zhang, Lei Zhang, Qiuyuan Huang, Xiaodong He, Siwei Lyu, and Jianfeng Gao. Object-driven text-to-image synthesis via adversarial training. In *CVPR*, 2019. **1, 5**
- [24] Jiadong Liang, Wenjie Pei, and Feng Lu. Cpgan: Full-spectrum content-parsing generative adversarial networks for text-to-image synthesis. *arXiv preprint arXiv:1912.08562*, 2019. **1, 3, 5, 6, 8, 11, 13**
- [25] Jae Hyun Lim and Jong Chul Ye. Geometric gan. *arXiv preprint arXiv:1705.02894*, 2017. **5**
- [26] Tsung-Yi Lin, Michael Maire, Serge Belongie, James Hays, Pietro Perona, Deva Ramanan, Piotr Dollár, and C Lawrence Zitnick. Microsoft coco: Common objects in context. In *ECCV*, 2014. **1, 6, 11, 12, 13, 16, 19**
- [27] Laurens van der Maaten and Geoffrey Hinton. Visualizing data using t-sne. *Journal of Machine Learning Research*, 9 (Nov), 2008. **12, 20, 21**
- [28] Xudong Mao, Q Li, H Xie, RYK Lau, and Z Wang. Least squares generative adversarial networks. cite. *arXiv preprint arXiv:1611.04076*, 2016. **5**
- [29] Mehdi Mirza and Simon Osindero. Conditional generative adversarial nets. *arXiv preprint arXiv:1411.1784*, 2014. **2**
- [30] Takeru Miyato and Masanori Koyama. cgans with projection discriminator. *arXiv preprint arXiv:1802.05637*, 2018. **5**
- [31] Takeru Miyato, Toshiki Kataoka, Masanori Koyama, and Yuichi Yoshida. Spectral normalization for generative adversarial networks. *arXiv preprint arXiv:1802.05957*, 2018. **5, 12, 13**

- [32] Mahdi Pakdaman Naeini, Gregory F Cooper, and Milos Hauskrecht. Obtaining well calibrated probabilities using bayesian binning. In *AAAI*, 2015. 4
- [33] Alexandru Niculescu-Mizil and Rich Caruana. Predicting good probabilities with supervised learning. In *ICML*, 2005. 4
- [34] M-E. Nilsback and A. Zisserman. Automated flower classification over a large number of classes. In *Proceedings of the Indian Conference on Computer Vision, Graphics and Image Processing*, Dec 2008. 1, 4
- [35] Augustus Odena, Christopher Olah, and Jonathon Shlens. Conditional image synthesis with auxiliary classifier gans. 2016. *Preprint at https://arxiv.org/abs/1610.09585*, 2016. 5
- [36] Tingting Qiao, Jing Zhang, Duanqing Xu, and Dacheng Tao. Mirrorgan: Learning text-to-image generation by redescription. In *CVPR*, 2019. 2
- [37] Alec Radford, Luke Metz, and Soumith Chintala. Unsupervised representation learning with deep convolutional generative adversarial networks. *arXiv preprint arXiv:1511.06434*, 2015. 5
- [38] Alec Radford, Jong Wook Kim, Chris Hallacy, Aditya Ramesh, Gabriel Goh, Sandhini Agarwal, Girish Sastry, Amanda Askell, Pamela Mishkin, Jack Clark, et al. Learning transferable visual models from natural language supervision. *arXiv preprint arXiv:2103.00020*, 2021. 2, 6, 7, 11
- [39] Aditya Ramesh, Mikhail Pavlov, Gabriel Goh, Scott Gray, Chelsea Voss, Alec Radford, Mark Chen, and Ilya Sutskever. Zero-shot text-to-image generation. In *ICML*, 2021. 2
- [40] Ali Razavi, Aaron van den Oord, and Oriol Vinyals. Generating diverse high-fidelity images with vq-vae-2. In *NeurIPS*, 2019. 2
- [41] Joseph Redmon and Ali Farhadi. Yolov3: An incremental improvement. *arXiv preprint arXiv:1804.02767*, 2018. 6
- [42] Scott Reed, Zeynep Akata, Xinchun Yan, Lajanugen Logeswaran, Bernt Schiele, and Honglak Lee. Generative adversarial text-to-image synthesis. In *ICML*, 2016. 2, 3, 5, 6, 8, 13
- [43] Olga Russakovsky, Jia Deng, Hao Su, Jonathan Krause, Sanjeev Satheesh, Sean Ma, Zhiheng Huang, Andrej Karpathy, Aditya Khosla, Michael Bernstein, et al. Imagenet large scale visual recognition challenge. *IJCV*, 115(3), 2015. 4
- [44] Tim Salimans, Ian Goodfellow, Wojciech Zaremba, Vicki Cheung, Alec Radford, and Xi Chen. Improved techniques for training gans. In *NeurIPS*, 2016. 1, 2, 5
- [45] Yujun Shen, Jinjin Gu, Xiaoou Tang, and Bolei Zhou. Interpreting the latent space of gans for semantic face editing. In *CVPR*, 2020. 1
- [46] Yujun Shen, Ceyuan Yang, Xiaoou Tang, and Bolei Zhou. Interfacegan: Interpreting the disentangled face representation learned by gans. *arXiv preprint arXiv:2005.09635*, 2020. 1
- [47] Christian Szegedy, Vincent Vanhoucke, Sergey Ioffe, Jon Shlens, and Zbigniew Wojna. Rethinking the inception architecture for computer vision. In *CVPR*, 2016. 2, 3
- [48] Hongchen Tan, Xiuping Liu, Xin Li, Yi Zhang, and Baocai Yin. Semantics-enhanced adversarial nets for text-to-image synthesis. In *ICCV*, 2019. 1, 2
- [49] Ming Tao, Hao Tang, Songsong Wu, Nicu Sebe, Fei Wu, Xiao-Yuan Jing, and Bingkun Bao. Df-gan: Deep fusion generative adversarial networks for text-to-image synthesis. *arXiv preprint arXiv:2008.05865*, 2020. 3, 5, 8, 13
- [50] Lucas Theis, Aäron van den Oord, and Matthias Bethge. A note on the evaluation of generative models. *arXiv preprint arXiv:1511.01844*, 2015. 2
- [51] Ashish Vaswani, Noam Shazeer, Niki Parmar, Jakob Uszkoreit, Llion Jones, Aidan N Gomez, Łukasz Kaiser, and Illia Polosukhin. Attention is all you need. In *NeurIPS*, 2017. 2
- [52] Peter Welinder, Steve Branson, Takeshi Mita, Catherine Wah, Florian Schroff, Serge Belongie, and Pietro Perona. Caltech-ucsd birds 200. Technical Report CNS-TR-2010-001, California Institute of Technology, 2010. 1, 3, 4, 12, 15, 19, 20, 21
- [53] Yan Wu, Jeff Donahue, David Balduzzi, Karen Simonyan, and Timothy Lillicrap. Logan: Latent optimisation for generative adversarial networks. *arXiv preprint arXiv:1912.00953*, 2019. 5
- [54] Tao Xu, Pengchuan Zhang, Qiuyuan Huang, Han Zhang, Zhe Gan, Xiaolei Huang, and Xiaodong He. Attngan: Fine-grained text to image generation with attentional generative adversarial networks. In *CVPR*, 2018. 1, 2, 3, 5, 8, 11, 12, 13, 17, 18
- [55] Hui Ye, Xiulong Yang, Martin Takac, Rajshekhar Sunderraman, and Shihao Ji. Improving text-to-image synthesis using contrastive learning. *arXiv preprint arXiv:2107.02423*, 2021. 2, 3, 5, 8, 13
- [56] Guojun Yin, Bin Liu, Lu Sheng, Nenghai Yu, Xiaogang Wang, and Jing Shao. Semantics disentangling for text-to-image generation. In *CVPR*, 2019. 1, 2
- [57] Han Zhang, Tao Xu, Hongsheng Li, Shaoting Zhang, Xiaogang Wang, Xiaolei Huang, and Dimitris N Metaxas. Stackgan: Text to photo-realistic image synthesis with stacked generative adversarial networks. In *ICCV*, 2017. 2, 3, 4, 8, 11, 13
- [58] Han Zhang, Tao Xu, Hongsheng Li, Shaoting Zhang, Xiaogang Wang, Xiaolei Huang, and Dimitris N Metaxas. Stackgan++: Realistic image synthesis with stacked generative adversarial networks. *TPAMI*, 41(8), 2018. 2, 3, 5

- [59] Han Zhang, Ian Goodfellow, Dimitris Metaxas, and Augustus Odena. Self-attention generative adversarial networks. In *ICML*, 2019. 5
- [60] Han Zhang, Jing Yu Koh, Jason Baldrige, Honglak Lee, and Yinfei Yang. Cross-modal contrastive learning for text-to-image generation. 2021. 2
- [61] Zizhao Zhang, Yuanpu Xie, and Lin Yang. Photographic text-to-image synthesis with a hierarchically-nested adversarial network. In *CVPR*, 2018. 5
- [62] Minfeng Zhu, Pingbo Pan, Wei Chen, and Yi Yang. Dm-gan: Dynamic memory generative adversarial networks for text-to-image synthesis. In *CVPR*, 2019. 1, 2, 3, 5, 8, 11, 13

## Supplementary Material

In this supplemental document, we provide additional details for the experiments conducted in the paper. We first provide the implementation details for the counter model to reproduce the IS metric’s inconsistency problem. We then present the comparison of our improved versions of RP and SOA to the original metrics to show how our metrics can mitigate the issues in the original versions in the multi-object case. We also show the statistical features of the test data we created. Furthermore, we provide a complete benchmark of multi-object text-to-image models based on each assessment criterion. As part of our contribution to the text-to-image approach, we also provide the architecture and network configurations of our AttnGAN++ as well as more visual examples and t-SNE visualization.

### A. Counter model implementation

This section details the development of our counter model, which was utilized to demonstrate the inconsistency problem of IS. Our counter model is built on AttnGAN++ and MSG-GAN [16]. Table 13 shows the network details of the counter model. The training and evaluation configurations can be found in Table 14. More random (not curated) visual samples synthesized by the counter model are also provided in Figure 9 to demonstrate that these samples from the counter model are quite poor in comparison to those from AttnGAN++.

### B. Mitigating overfitting phenomenon in RP and SOA

In the main paper, we presented that the existing versions of RP and SOA overfit in the multi-object scenario of the MS-COCO dataset, as evidenced by the fact that the values from some methods on these metrics exceed the corresponding values from real photos although these methods produce

images with poorer quality than real photos. We demonstrate this by comparing the values of the original and our modified versions of these metrics in Table 7 and Table 8. As can be seen, the overfitting phenomena on RP and SOA is fully eliminated in our enhanced versions.

Method	R-precision (original) ( $\uparrow$ )	R-precision (ours) ( $\uparrow$ )
StackGAN [57]	<b>72.03</b>	38.46
AttnGAN [54]	<b>83.76</b>	50.92
DM-GAN [62]	<b>92.23</b>	65.91
CPGAN [24]	<b>93.59</b>	70.36
AttnGAN++ (ours)	<b>96.39</b>	73.37
Real Images	67.35	83.65

Table 7. Comparison of the original version of RP and our improved version one on the MS-COCO [26] dataset. Inconsistent results are marked in **bold**. As can be observed, the value of RP on real photographs is the lowest, showing the original RP’s heavily overfitting issue. Noticeably, our improved RP alleviated significantly by using CLIP [38]. Note that the values of RP in these experiments are calculated from 30,000 captions as most of the previous works do. In the main paper, we only sample 5,000 captions and calculate RP from these captions to save time but guarantee consistent scores.

Method	SOA-C ( $\uparrow$ ) (original)	SOA-I ( $\uparrow$ ) (original)	SOA-C ( $\uparrow$ ) (ours)	SOA-I ( $\uparrow$ ) (ours)
StackGAN [57]	21.09	30.35	31.34	49.97
AttnGAN [54]	25.88	39.01	47.26	62.02
DM-GAN [62]	33.44	48.03	55.40	68.76
CPGAN [24]	<b>77.02</b>	<b>84.55</b>	82.25	88.97
AttnGAN++(ours)	48.33	67.19	67.52	76.33
Real Images	74.97	80.84	89.98	92.92

Table 8. Comparison of the original version of SOA (including SOA-I and SOA-C) and our improved version of SOA on the MS-COCO [26] dataset. Inconsistent results are highlighted in **bold**, which shows that SOA-C and SOA-I of CPGAN are higher than real images and our SOA greatly migrated this phenomenon. Note that the values of SOA in this experiment are calculated on full captions provided by the authors of this metric, while the ones we report by our TISE toolbox are computed on the sample from them (about 16k captions) to save time but output the consistent scores.

### C. Details of the evaluation data for our benchmark

In the previous works, the inconsistency in the construction of testing data has caused many difficulties in benchmark models. A comprehensive survey [6] also pointed that there are some metrics are reported with inconsistent numbers between different research works. We find out that the non-unified input test data is one of the reasons leading to this issue. Therefore, we provide unified testing data in our TISE toolset in order to compare techniques fairly. We

Metric	#Captions
Image Realism (IS, FID)	30,000
Text Relevance (RP)	30,000

Table 9. The number of test captions used in evaluation on the CUB dataset.

Metric	#Captions
Image Realism (IS, FID)	10,000
Object Fidelity (O-IS, O-FID)	10,000
Text Relevance (RP)	5,000
Object Accuracy (SOA-C, SOA-I)	15,223
Positional Alignment (PA)	1,046
Counting Alignment (CA)	1,000

Table 10. The number of test captions used in evaluating each evaluation aspect on the MSCOCO dataset.

would release them officially along with TISE upon paper acceptance.

The details of our test data is as follows. The number of captions used in each metrics are shown in Table 9 and Table 10 for CUB and MS-COCO, respectively. The distribution of per-class object count and positional words for counting alignment (CA) and positional alignment (PA) metric are visualized in Figure 6 and Figure 7, respectively.

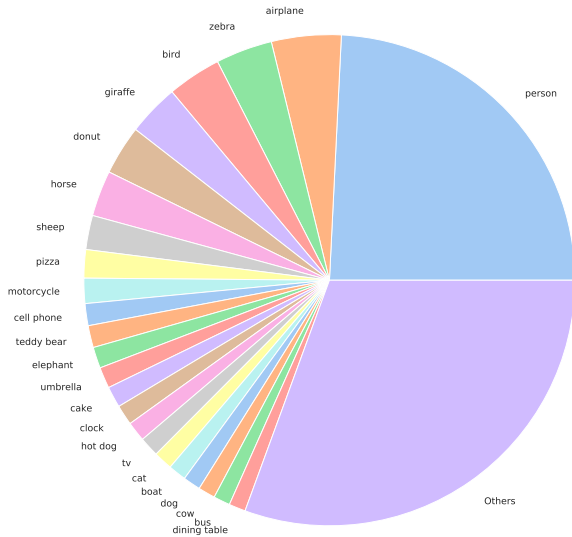


Figure 6. Distribution of the number of object classes in our provided testing data for counting alignment factor in multi-object case. Best viewed in zoom.

### C.1. Ranking scores for each evaluation aspect

Table 11 provides the details of aspect ranking scores for each method to show the performance of the model on

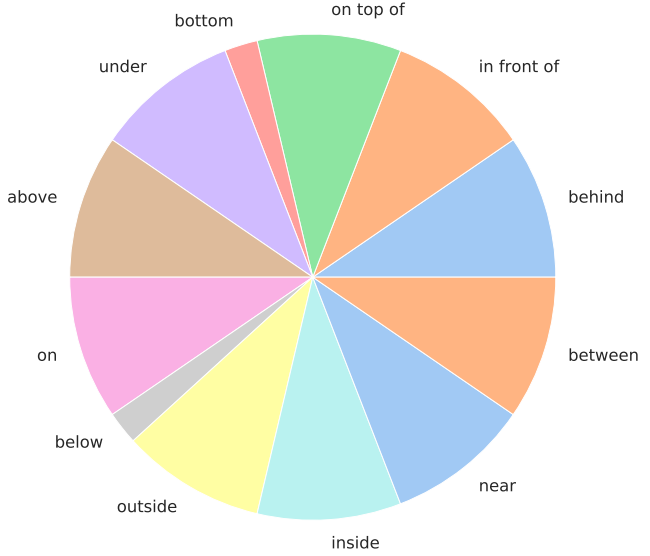


Figure 7. Distribution of the number of test captions having corresponding positional words considered in our PA metric.

six evaluation criteria, including Image Realism, Object Accuracy, Text Relevance, Object Accuracy, Object Fidelity, Counting Alignment, Positional Alignment.

## D. AttnGAN++ Architecture

Along with the assessment toolkit, we also offered our AttnGAN++, a new baseline based on AttnGAN [54]. The main difference between AttnGAN++ and AttnGAN is that we apply spectral normalization [31] to discriminators to stabilize the training process of GAN. With this simple technique, the performance of the model is boosted significantly comparing with the original version. The architecture of AttnGAN++ is shown in Figure 8. The network details and training settings of AttnGAN++ are demonstrated in Table 12 and Table 14 respectively. Additionally, we show more visual examples of our AttnGAN++ comparing with the current state-of-the-art text-to-image models on CUB [52] dataset in Figure 10 and MS-COCO [26] dataset in Figure 11 for qualitative measuring.

### D.1. t-SNE Visualizations

To visualize the statistics of synthesized images, we utilize t-SNE [27]. Firstly, we extract feature vectors from these synthesized images using a pre-trained image encoder [54]. Then, we use t-SNE to convert these high dimensional feature vectors to 2-dimensional positions at which we display the images. The t-SNE visualization of generated images by AttnGAN++ on CUB can be found in Figure 12. Additionally, we also show the t-SNE of all real images of the CUB test set in Figure 13 for reference.

Method	Image Realism	Text Relevance	Object Accuracy	Object Fidelity	Counting Alignment	Positional Alignment
GAN-CLS [42]	1.0	2.0	1.0	1.0	1.0	1.0
StackGAN [57]	2.5	1.0	2.0	2.0	2.0	2.0
AttnGAN [54]	5.0	5.0	5.5	5.0	6.0	3.0
DM-GAN [62]	6.5	7.0	7.0	7.5	8.0	5.0
CPGAN [24]	7.5	8.0	<b>10.0</b>	7.5	4.0	6.0
DF-GAN [49]	5.5	3.0	4.0	6.0	5.0	4.0
AttnGAN + CL [55]	7.0	6.0	5.5	5.5	7.0	7.0
DM-GAN + CL [55]	<u>9.0</u>	<u>9.0</u>	8.0	<u>8.0</u>	<u>9.0</u>	<b>10.0</b>
DALLE-mini (zero-shot) [4]	2.5	4.0	3.0	3.0	3.0	8.0
AttnGAN++ (Ours)	<b>9.5</b>	<b>10.0</b>	<u>9.0</u>	<b>9.5</b>	<b>10.0</b>	<u>9.0</u>
<i>Real Images</i>	<i>10.0</i>	<i>11.0</i>	<i>11.0</i>	<i>11.0</i>	<i>11.0</i>	<i>11.0</i>

Table 11. The details of the ranking scores for each evaluation aspect of each method on the MS-COCO [26] dataset. **Best** and runner-up values are marked in bold and underline, respectively.

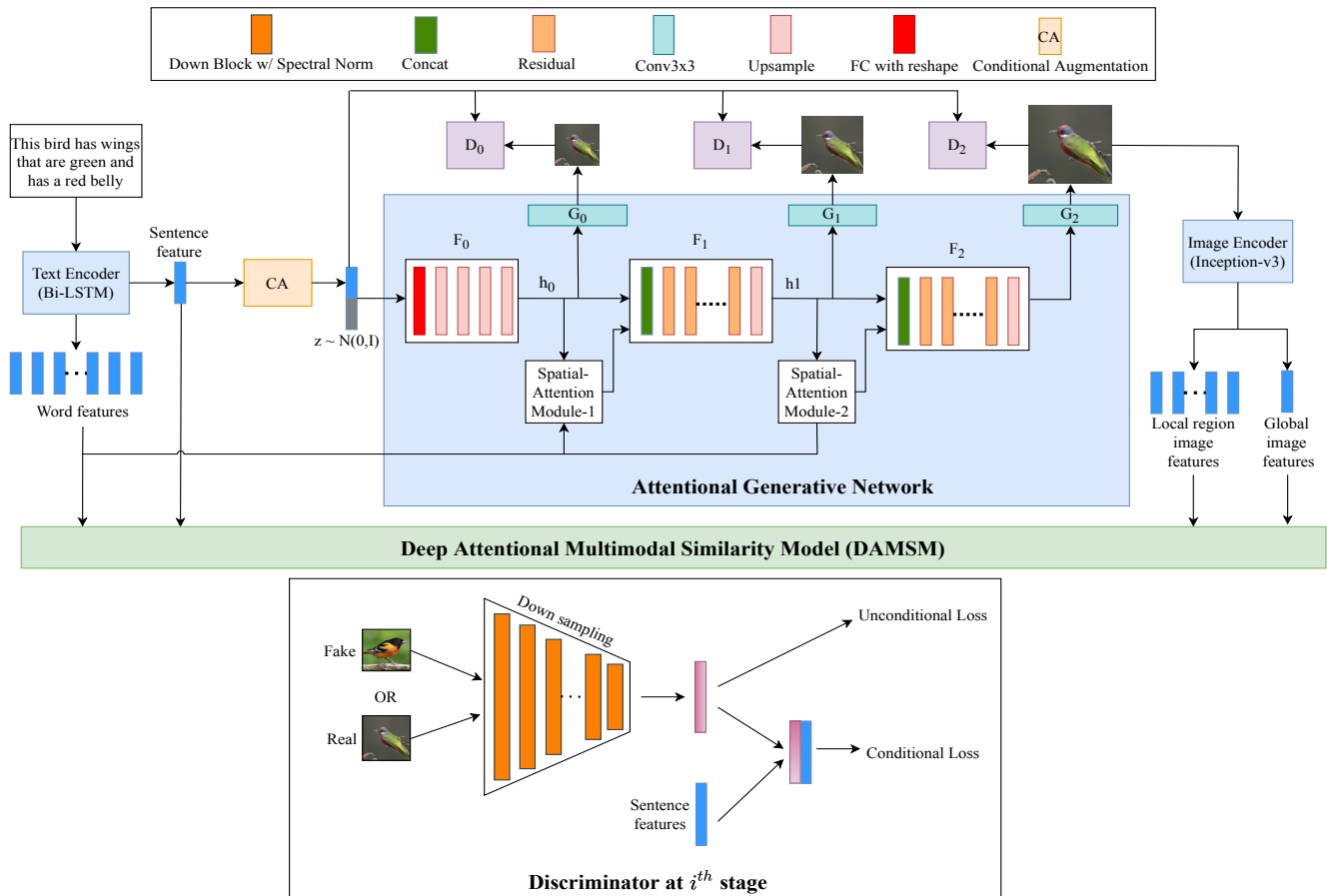


Figure 8. The architecture of our AttnGAN++. In each discriminator, we employ spectral normalization [31] to each convolution layer instead of using batch normalization [14] as in the original AttnGAN [54]. Implementation details for each layer can be found in Table 12.

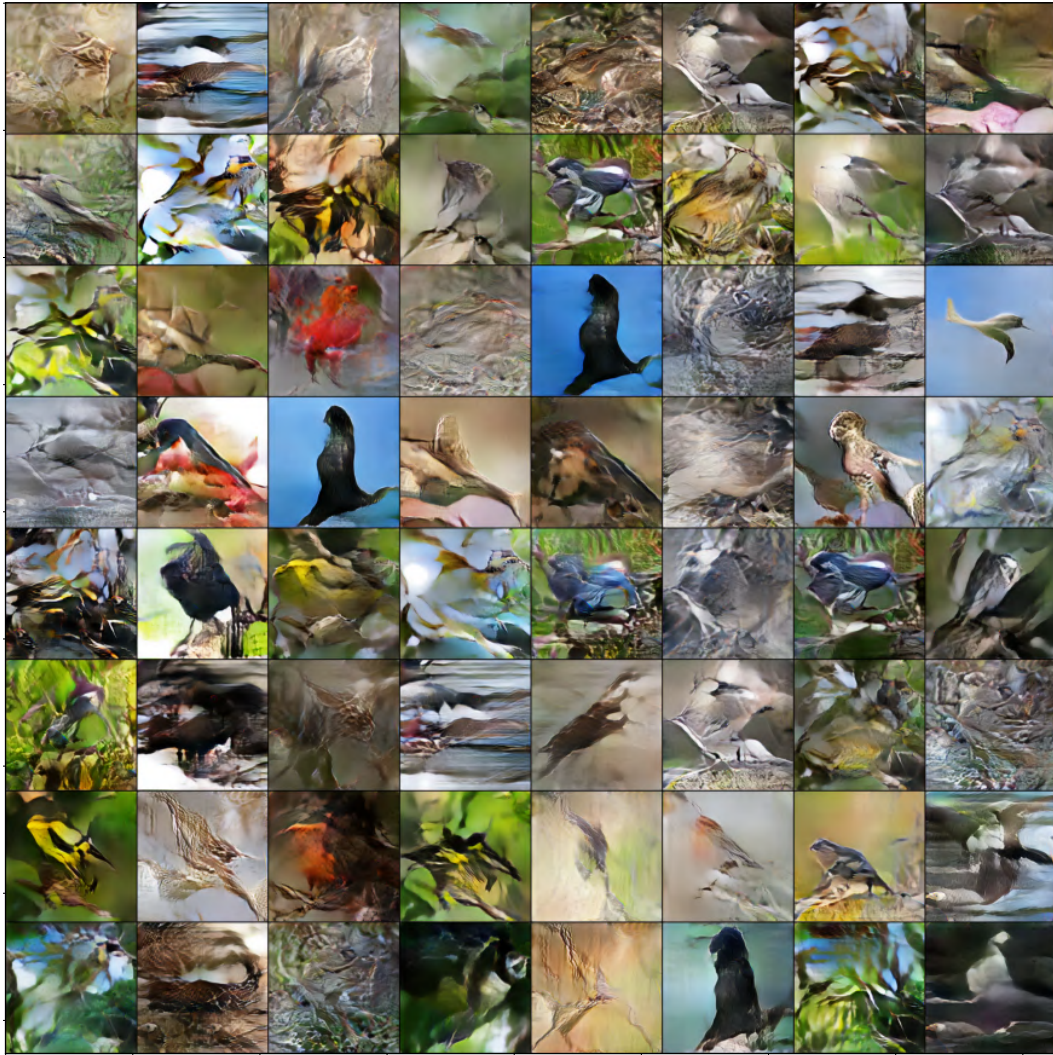


Figure 9. More random (not curated) visual samples from our countermodel on the CUB dataset. As can be seen, the synthesized images are not realistic in most cases.



Figure 10. Qualitative examples of the single object text-to-image generation models on the CUB [52] dataset. Best viewed in zoom.

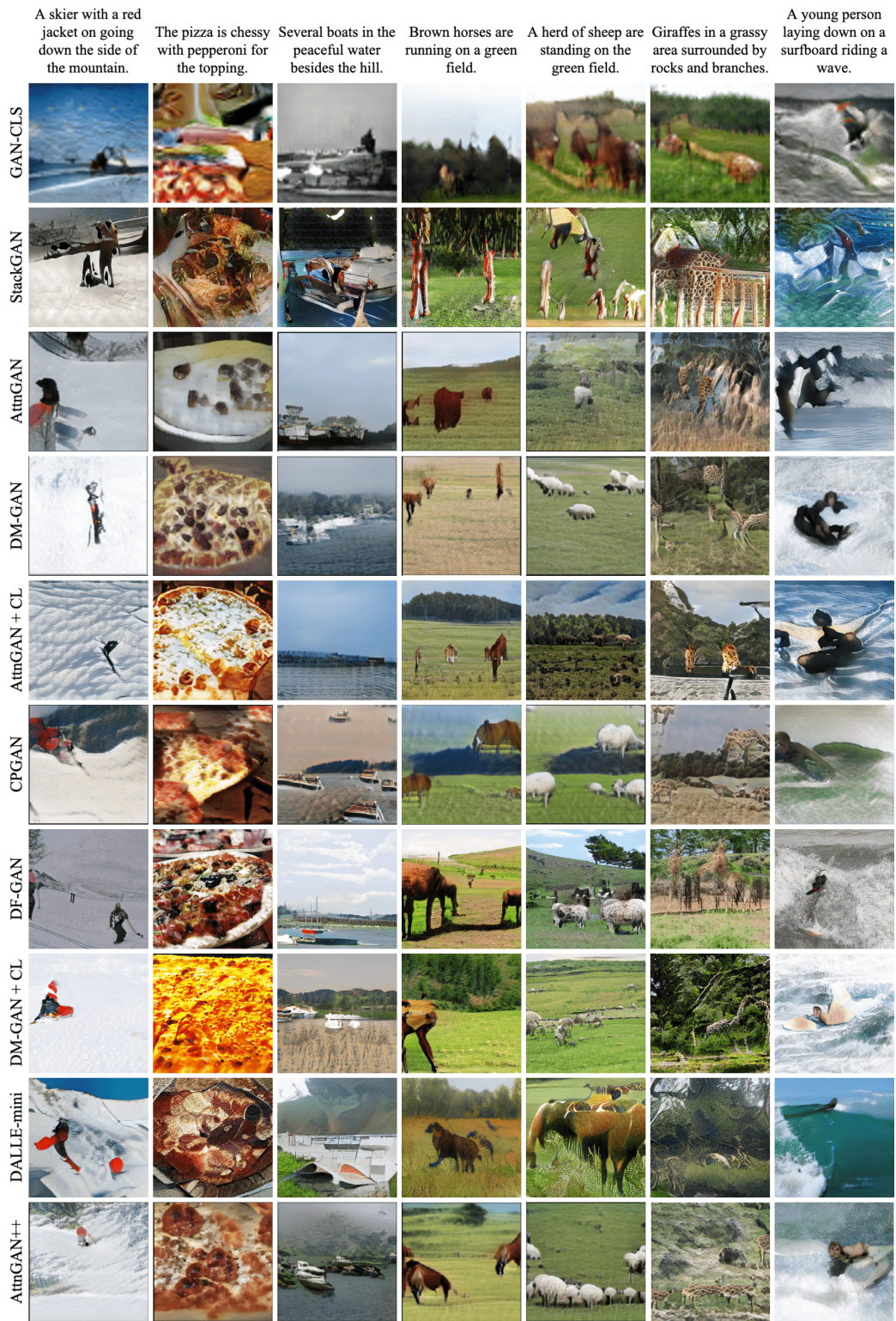


Figure 11. Qualitative examples of the multi-object text-to-image synthesis models on the MS-COCO [26] dataset. Best viewed in zoom.



Module	Output shape / Details
<b>Up Block</b>	
<i>Params:</i> (in_planes, out_planes)	
Input shape	in_planes $\times$ h $\times$ w
Upsampling	Nearest Neighbor, scale factor = 2
Conv(k=3, s=1, p=1, b=False)	2 * out_planes $\times$ h * 2 $\times$ w * 2
BatchNorm2D	No change shape
Gated Linear Unit (GLU)	out_planes $\times$ h * 2 $\times$ w * 2
<b>Residual Block</b>	
Input X	
Conv(k=3, s=1, p=1, b=False)	Up channel size by 2,
BatchNorm2D	No change shape
Gated Linear Unit (GLU)	Down channel size by 2
Conv(k=3, s=1, p=1, b=False)	No change shape
BatchNorm2D	No change shape
Add output w/ X (skip connection)	No change shape
<b>Spatial Attention layer</b>	see AttnGAN
<b>Conditional Augmentation (CA)</b>	see AttnGAN
<b>Generator</b> 64 $\times$ 64	
<i>Input</i>	
Input noise	<i>nzf</i>
Caption Embedding	<i>nef</i>
<i>Computation</i>	
CA on caption embedding to get c	<i>ncf</i>
Concat c w/ noise	<i>ncf + nzf</i>
Linear(b=False)	<i>ngf</i> * 16 * 4 * 4 * 2
BatchNorm1D	No change shape
Gated Linear Unit (GLU)	<i>ngf</i> * 16 * 4 * 4 * 1
Reshape	16 * <i>ngf</i> $\times$ 4 $\times$ 4
Up Block 1	8 * <i>ngf</i> $\times$ 8 $\times$ 8
Up Block 2	4 * <i>ngf</i> $\times$ 16 $\times$ 16
Up Block 3	2 * <i>ngf</i> $\times$ 32 $\times$ 32
Up Block 4	<i>ngf</i> $\times$ 64 $\times$ 64
Conv(k=3, s=1, p=1, b=False)	3 $\times$ 64 $\times$ 64
Tanh	No change shape
<b>Generator</b> 128 $\times$ 128	
<i>Input</i>	
Previous hidden features	<i>ngf</i> $\times$ 64 $\times$ 64
Word Mask	<i>word_num</i>
Word features	<i>nef</i> $\times$ <i>word_num</i>
<i>Computation</i>	
Spatial Attention Layer	<i>ngf</i> $\times$ 64 $\times$ 64
Residual Block $\times$ residual_num	<i>ngf</i> $\times$ 64 $\times$ 64
Concat w/ previous hidden features	2 * <i>ngf</i> $\times$ 64 $\times$ 64
Up Block	<i>ngf</i> $\times$ 128 $\times$ 128
Conv(k=3, s=1, p=1, b=False)	3 $\times$ 128 $\times$ 128
Tanh	No change shape
<b>Generator</b> 256 $\times$ 256	
<i>Input</i>	
Previous hidden features	<i>ngf</i> $\times$ 128 $\times$ 128
Word Mask	<i>word_num</i>
Word features	<i>nef</i> $\times$ <i>word_num</i>
<i>Computation</i>	
Spatial Attention Layer	<i>ngf</i> $\times$ 128 $\times$ 128
Residual Block $\times$ residual_num	<i>ngf</i> $\times$ 128 $\times$ 128
Concat w/ previous hidden features	2 * <i>ngf</i> $\times$ 128 $\times$ 128
Up Block	<i>ngf</i> $\times$ 256 $\times$ 256
Conv(k=3, s=1, p=1, b=False)	3 $\times$ 256 $\times$ 256
Tanh	No change shape

(a) Generator

Module	Output shape / Details
<b>Down Block</b>	
<i>Params:</i> (in_planes, out_planes)	
Input shape	in_planes $\times$ h $\times$ w
SpectralNorm(Conv(k=4, s=2, p=1, b=True))	out_planes $\times$ h/2 $\times$ w/2
LeakyReLU(alpha=0.2)	No change shape
<b>Block3x3_leakyReLU</b>	
<i>Params:</i> (in_planes, out_planes)	
Input shape	in_planes $\times$ h $\times$ w
SpectralNorm(Conv(k=3, s=1, p=1, b=True))	out_planes $\times$ h $\times$ w
LeakyReLU(alpha=0.2)	No change shape
<b>Discriminator</b> 256 $\times$ 256	
Input tensor	3 $\times$ 256 $\times$ 256
Down Block	<i>ndf</i> $\times$ 128 $\times$ 128
Down Block	2 * <i>ndf</i> $\times$ 64 $\times$ 64
Down Block	4 * <i>ndf</i> $\times$ 32 $\times$ 32
Down Block	8 * <i>ndf</i> $\times$ 16 $\times$ 16
Down Block	16 * <i>ndf</i> $\times$ 8 $\times$ 8
Down Block	32 * <i>ndf</i> $\times$ 4 $\times$ 4
Block3x3_leakyReLU	16 * <i>ndf</i> $\times$ 4 $\times$ 4
Block3x3_leakyReLU	8 * <i>ndf</i> $\times$ 4 $\times$ 4
<i>Unconditional logits</i>	
Conv(k=4, s=4, p=0, b=True)	1
Sigmoid	1
<i>Conditional logits</i>	
Caption Embedding	<i>nef</i>
Concat w/ replicated caption embedding	8 * <i>ndf</i> + <i>nef</i> $\times$ 4 $\times$ 4
Block3x3_leakyReLU	8 * <i>ndf</i> $\times$ 4 $\times$ 4
Conv(k=4, s=4, p=0, b=True)	1
Sigmoid	1
<b>Discriminator</b> 128 $\times$ 128	
Input tensor	3 $\times$ 128 $\times$ 128
Down Block	<i>ndf</i> $\times$ 64 $\times$ 64
Down Block	2 * <i>ndf</i> $\times$ 32 $\times$ 32
Down Block	4 * <i>ndf</i> $\times$ 16 $\times$ 16
Down Block	8 * <i>ndf</i> $\times$ 8 $\times$ 8
Down Block	16 * <i>ndf</i> $\times$ 4 $\times$ 4
Block3x3_leakyReLU	8 * <i>ndf</i> $\times$ 4 $\times$ 4
<i>Unconditional logits</i>	
Conv(k=4, s=4, p=0, b=True)	1
Sigmoid	1
<i>Conditional logits</i>	
Caption Embedding	<i>nef</i>
Concat w/ replicated caption embedding	8 * <i>ndf</i> + <i>nef</i> $\times$ 4 $\times$ 4
Block3x3_leakyReLU	8 * <i>ndf</i> $\times$ 4 $\times$ 4
Conv(k=4, s=4, p=0, b=True)	1
Sigmoid	1
<b>Discriminator</b> 64 $\times$ 64	
Input tensor	3 $\times$ 64 $\times$ 64
Down Block	<i>ndf</i> $\times$ 32 $\times$ 32
Down Block	2 * <i>ndf</i> $\times$ 16 $\times$ 16
Down Block	4 * <i>ndf</i> $\times$ 8 $\times$ 8
Down Block	8 * <i>ndf</i> $\times$ 4 $\times$ 4
<i>Unconditional logits</i>	
Conv(k=4, s=4, p=0, b=True)	1
Sigmoid	1
<i>Conditional logits</i>	
Caption Embedding	<i>nef</i>
Concat w/ replicated caption embedding	8 * <i>ndf</i> + <i>nef</i> $\times$ 4 $\times$ 4
Block3x3_leakyReLU	8 * <i>ndf</i> $\times$ 4 $\times$ 4
Conv(k=4, s=4, p=0, b=True)	1
Sigmoid	1

(b) Discriminator

Table 12. Network details of our AttnGAN++. Some components which are not mentioned here such as text encoder, image encoder, DAMSM, its settings can be found in AttnGAN [54]. In the tables, k = kernel size, s = stride, p = padding, b = bias.

Module	Output shape / Details
<b>Up Block</b>	see Table 12a
<b>Residual Block</b>	see Table 12a
<b>Spatial Attention Layer</b>	see AttnGAN
<b>Conditional Augmentation</b>	see AttnGAN
<b>Generator</b> $4 \times 4$	
<i>Input</i>	
Input noise	$nzf$
Caption Embedding	$nef$
<i>Computation</i>	
Conditional Augmentation on caption embedding	$ncf$
Concat w/ noise	$ncf + nef$
Linear(b=False)	$ngf * 16 * 4 * 4 * 2$
BatchNorm1D	No change shape
Gated Linear Unit (GLU)	$ngf * 16 * 4 * 4 * 1$
Reshape	$16 * ngf \times 4 \times 4$
Conv(k=3, s=1, p=1, b=False)	$3 \times 4 \times 4$
Tanh	No change shape
<b>Generator</b> $8 \times 8$	
Up Block	$8 * ngf \times 8 \times 8$
Conv(k=3, s=1, p=1, b=False)	$3 \times 8 \times 8$
Tanh	No change shape
<b>Generator</b> $16 \times 16$	
Up Block	$4 * ngf \times 16 \times 16$
Conv(k=3, s=1, p=1, b=False)	$3 \times 16 \times 16$
Tanh	No change shape
<b>Generator</b> $32 \times 32$	
Up Block	$2 * ngf \times 32 \times 32$
Conv(k=3, s=1, p=1, b=False)	$3 \times 32 \times 32$
Tanh	No change shape
<b>Generator</b> $64 \times 64$	
Up Block	$ngf \times 64 \times 64$
Conv(k=3, s=1, p=1, b=False)	$3 \times 64 \times 64$
Tanh	No change shape
<b>Generator</b> $128 \times 128$	
<i>Input</i>	
Previous hidden features	$ngf \times 64 \times 64$
Word Mask	$word\_num$
Word features	$nef \times word\_num$
<i>Computation</i>	
Spatial Attention Layer	$ngf \times 64 \times 64$
Residual Block $\times$ residual_num	$ngf \times 64 \times 64$
Concat w/ previous hidden features	$2 * ngf \times 64 \times 64$
Up Block $ngf \times 128 \times 128$	
Conv(k=3, s=1, p=1, b=False)	$3 \times 128 \times 128$
Tanh	No change shape
<b>Generator</b> $256 \times 256$	
<i>Input</i>	
Previous hidden features	$ngf \times 128 \times 128$
Word Mask	$word\_num$
Word features	$nef \times word\_num$
<i>Computation</i>	
Spatial Attention Layer	$ngf \times 128 \times 128$
Residual Block $\times$ residual_num	$ngf \times 128 \times 128$
Concat w/ previous hidden features	$2 * ngf \times 128 \times 128$
Up Block	$ngf \times 256 \times 256$
Conv(k=3, s=1, p=1, b=False)	$3 \times 256 \times 256$
Tanh	No change shape

(a) Generator

Module	Output shape / Details
<b>Block3x3_LeakyReLU</b>	see Table 12b
<b>DisGeneralConvBlock</b>	
<i>Params: in_planes, concat_planes, out_planes</i>	
MinibatchStdDev (see [17, 18])	$in\_planes + concat\_planes \times h \times w$
Block3x3_LeakyRelu	$in\_planes \times h \times w$
Block3x3_LeakyRelu	$out\_planes \times h \times w$
AvgPool2d(k=2)	$out\_planes \times h/2 \times w/2$
<b>Discriminator</b>	
<i>Input</i>	
Caption Embedding	$nef$
Image scale $4 \times 4$	$3 \times 4 \times 4$
Image scale $8 \times 8$	$3 \times 8 \times 8$
Image scale $16 \times 16$	$3 \times 16 \times 16$
Image scale $32 \times 32$	$3 \times 32 \times 32$
Image scale $64 \times 64$	$3 \times 64 \times 64$
Image scale $128 \times 128$	$3 \times 128 \times 128$
Image scale $256 \times 256$	$3 \times 256 \times 256$
<i>Computation</i>	
Image scale $256 \times 256$	$3 \times 256 \times 256$
Conv(k=1, s=1, p=0, b=True)	$ndf \times 256 \times 256$
DisGeneralConvBlock( $ndf, 1, 2 * ndf$ )	$ndf * 2 \times 128 \times 128$
Concat w/ Image scale $128 \times 128$	$ndf * 2 + 3 \times 128 \times 128$
DisGeneralConvBlock( $2 * ndf, 4, 4 * ndf$ )	$4 * ndf \times 64 \times 64$
Concat w/ Image scale $64 \times 64$	$4 * ndf + 3 \times 64 \times 64$
DisGeneralConvBlock( $4 * ndf, 4, 8 * ndf$ )	$8 * ndf \times 32 \times 32$
Concat w/ Image scale $32 \times 32$	$8 * ndf + 3 \times 32 \times 32$
DisGeneralConvBlock( $8 * ndf, 4, 8 * ndf$ )	$8 * ndf \times 16 \times 16$
Concat w/ Image scale $16 \times 16$	$8 * ndf + 3 \times 16 \times 16$
DisGeneralConvBlock( $8 * ndf, 4, 8 * ndf$ )	$8 * ndf \times 8 \times 8$
Concat w/ Image scale $8 \times 8$	$8 * ndf + 3 \times 8 \times 8$
DisGeneralConvBlock( $8 * ndf, 4, 8 * ndf$ )	$8 * ndf \times 4 \times 4$
<i>Unconditional logits</i>	
Conv(k=4, s=4, p=0, b=True)	1
Sigmoid	1
<i>Conditional logits</i>	
Caption Embedding	$nef$
Concat w/ replicated caption embedding	$8 * ndf + nef \times 4 \times 4$
Block3x3_LeakyReLU	$8 * ndf \times 4 \times 4$
Conv(k=4, s=4, p=0, b=True)	1
Sigmoid	1

(b) Discriminator

Table 13. Network details of our countermodel. Some components which are not mentioned here such as text encoder, image encoder, DAMSM, its settings can be found in AttnGAN [54]. In the tables, k = kernel size, s = stride, p = padding, b = bias.

Dataset	CUB [52]	MS-COCO [26]
Optimizer	Adam( $\beta_1 = 0.5, \beta_2 = 0.999$ )	Adam( $\beta_1 = 0.5, \beta_2 = 0.999$ )
Generator (G) Learning Rate	0.0002	0.0002
Discriminator (D) Learning Rate	0.0002	0.0002
G/D Update	1 : 1	1 : 1
$\gamma_1$	4.0	4.0
$\gamma_2$	5.0	5.0
$\gamma_3$	10.0	10.0
$\lambda$	5.0	50.0
residual_num	2	3
ngf	64	64
ndf	32	32
nef	256	256
nzf	100	100
ncf	100	100
max_epochs	800	200
word_num	18	12

Table 14. Training settings of both AttnGAN++ and counter model. Most of settings in evaluation process is the same with training process except word\_num. In the evaluation process, word\_num=25 for the CUB [52] dataset and word\_num=20 for the MS-COCO [26] dataset.

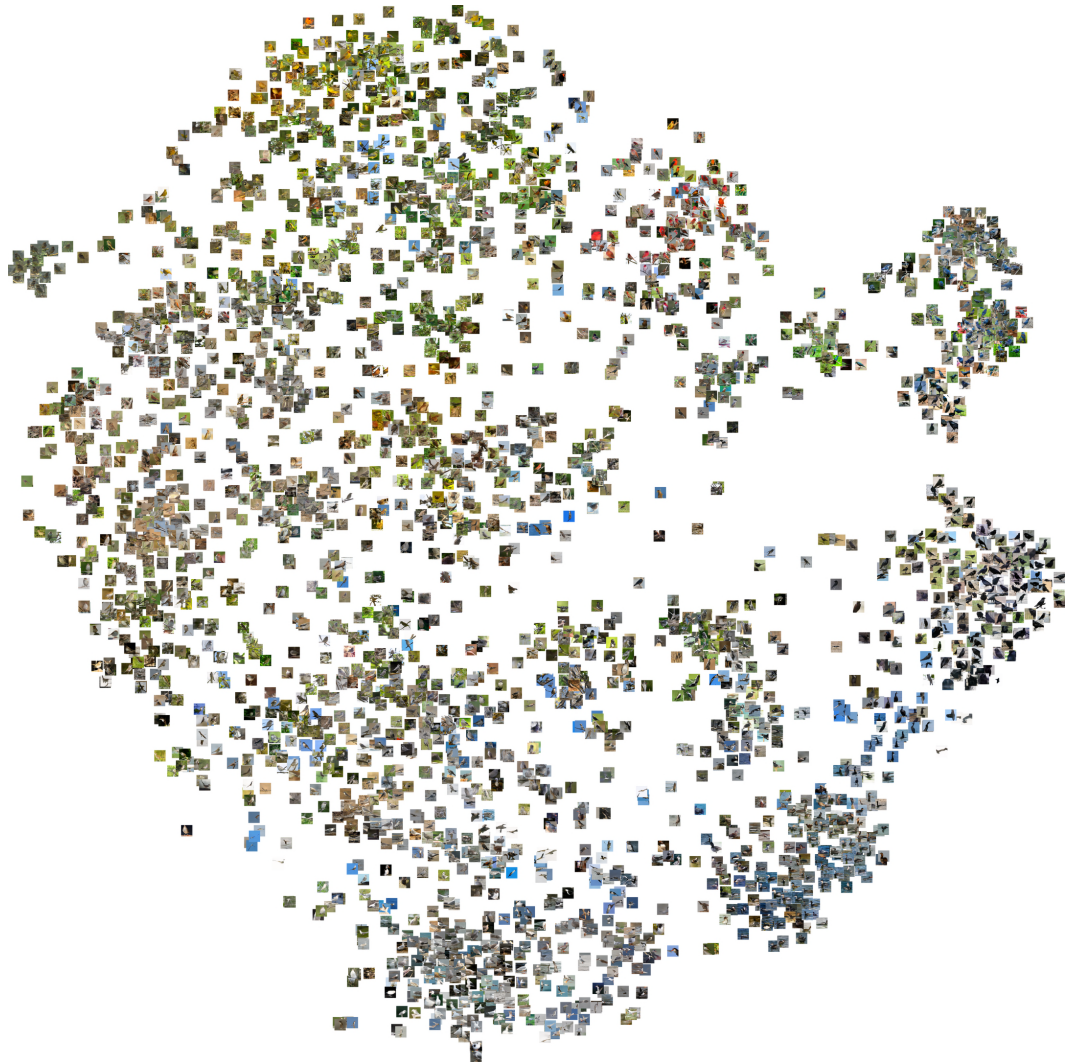


Figure 12. Visualization of generated images from captions on the test set of CUB [52] dataset by **our AttnGAN++** using t-SNE [27]. The number of clusters in the visualization shows that the photos generated by our model span a wide range of bird species. As a result of the similar appearances of various bird species, some clusters are near together and overlap slightly. We also found no intra-class mode dropping, indicating that the model does not create the same sample in each bird class over and over. As can be seen in each cluster, the samples are belonging to one bird class with a variety of poses, and backgrounds. Best viewed in zoom.

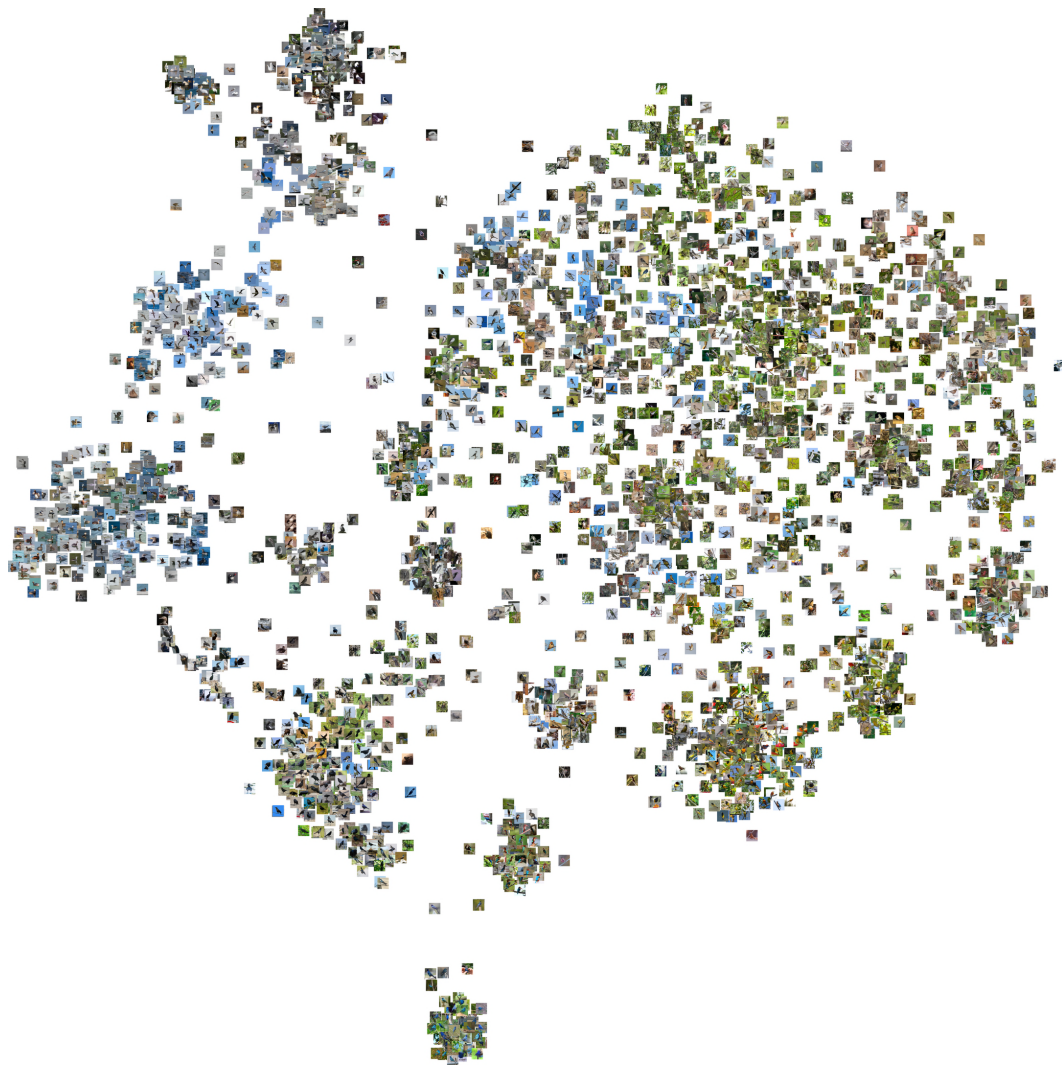


Figure 13. Visualization of **real images** from CUB [52] test set by using t-SNE [27]. Best viewed in zoom.